PROCEEDINGS OF SCIENCE

arXiv:0908.4584v1 [hep-ex] 31 Aug 2009

Test of lepton flavor violation with Ke2 decay at KLOE

Barbara Sciascia[*†]
LNF-INFN
E-mail: barbara.sciascia@lnf.infn.it

We present a precise measurement of the ratio $R_K = \Gamma(K \to e\nu(\gamma))/\Gamma(K \to \mu\nu(\gamma))$ performed with the KLOE detector. The results are based on data collected at the Frascati e^+e^- collider DA$\breve{}$NE for an integrated luminosity of 2.2 fb^{-1}. We find $R_K = (2.493 \pm 0.025_{\rm stat} \pm 0.019_{\rm syst}) \times 10^{-5}$, in agreement with the Standard Model expectation. This result is used to improve constraints on parameters of the Minimal Supersymmetric Standard Model with lepton flavor violation.

2009 KAON International Conference KAON09,
June 09 - 12 2009
Tsukuba, Japan

[*]Speaker.

[†]for the KLOE Collaboration: F. Ambrosino, A. Antonelli, M. Antonelli, F. Archilli, P. Beltrame, G. Bencivenni, C. Bini, C. Bloise, S. Bocchetta, F. Bossi, P. Branchini, G. Capon, D. Capriotti, T. Capussela, F. Ceradini, P. Ciambrone, E. De Lucia, A. De Santis, P. De Simone, G. De Zorzi, A. Denig, A. Di Domenico, C. Di Donato, B. Di Micco, M. Dreucci, G. Felici, S. Fiore, P. Franzini, C. Gatti, P. Gauzzi, S. Giovannella, E. Graziani, M. Jacewicz, V. Kulikov, G. Lanfranchi, J. Lee-Franzini, M. Martini, P. Massarotti, S. Meola, S. Miscetti, M. Moulson, S. Müller, F. Murtas, M. Napolitano, F. Nguyen, M. Palutan, A. Passeri, V. Patera, P. Santangelo, B. Sciascia, A. Sibidanov, T. Spadaro, M. Testa, L. Tortora, P. Valente, G. Venanzoni, and R. Versaci.

© Copyright owned by the author(s) under the terms of the Creative Commons Attribution-NonCommercial-ShareAlike Licence.

The decay $K^{\pm} \to e^{\pm}\nu$ is strongly suppressed, $\sim$few$\times 10^{-5}$, because of conservation of angular momentum and the vector structure of the charged weak current. It therefore offers the possibility of detecting minute contributions from physics beyond the Standard Model (SM). This is particularly true of the ratio $R_K = \Gamma(K \to e\nu)/\Gamma(K \to \mu\nu)$ which, in the SM, is calculable without hadronic uncertainties [1, 2]. Physics beyond the SM, for example multi-Higgs effects inducing an effective pseudo-scalar interaction, can change the value of R_K. It has been shown in Ref. [3] that deviations of R_K of up to *a few percent* are possible in minimal supersymmetric extensions of the SM (MSSM) with non vanishing e-τ scalar lepton mixing. To obtain accurate predictions, the radiative process $K \to e\nu\gamma$ ($K_{e2\gamma}$) must be included. In $K_{e2\gamma}$, photons can be produced via internal-bremsstrahlung (IB) or direct-emission (DE), the latter being dependent on the hadronic structure. Interference among the two processes is negligible [4]. The DE contribution to the total width is approximately equal to that of IB [4] but is presently known with a 15% fractional accuracy [5].

R_K is *defined* to be inclusive of IB, ignoring however DE contributions. A recent calculation [2], which includes order e^2p^4 corrections in chiral perturbation theory (χPT), gives:

$$R_K = (2.477 \pm 0.001) \times 10^{-5}. \tag{1}$$

R_K is not directly measurable, since IB cannot be distinguished from DE on an event-by-event basis. Therefore, in order to compare data with the SM prediction at the percent level or better, one has to be careful with the DE part. We define the rate R_{10} as:

$$R_{10} = \Gamma(K \to e\nu(\gamma),\ E_\gamma < 10\ \text{MeV})/\Gamma(K \to \mu\nu). \tag{2}$$

Evaluating the IB spectrum to $\mathcal{O}(\alpha_{\text{em}})$ with resummation of leading logarithms, R_{10} includes $93.57 \pm 0.07\%$ of the IB,

$$R_{10} = R_K \times (0.9357 \pm 0.0007). \tag{3}$$

The DE contribution in this range is expected to be negligible. R_{10} is measured without photon detection. Some small contribution of DE is present in the selected sample. In particular, DE decays have some overlap with the IB emission at high p_e. We have also measured [7] the differential width $\mathrm{d}R_\gamma/\mathrm{d}E_\gamma$ for $E_\gamma > 10$ MeV and $p_e > 200$ MeV requiring photon detection, both to test χPT predictions for the DE terms and to reduce possible systematic uncertainties on the R_{10} measurement.

1. Selection of leptonic kaon decays

$K^{\pm}$ decays are signaled by the observation of two tracks with the following conditions. One track must originate at the interaction point (IP) and have momentum in the interval $\{70, 130\}$ MeV, consistent with being a kaon from ϕ-decay. The second track must originate at the end of the previous track and have momentum larger than that of the kaon, with the same charge. The second track is taken as a decay product of the kaon. The point of closest approach of the two tracks is taken as the kaon decay point D and must satisfy $40 < r_{\text{D}} < 150$ cm, $|z_{\text{D}}| < 80$ cm. The geometrical acceptance with these conditions is $\sim$56%, while the decay point reconstruction efficiency is $\sim$51%. From the measured kaon and decay particle momenta, $\mathbf{p}_K$ and $\mathbf{p}_{\text{d}}$, we compute the squared mass m_ℓ^2 of the lepton for the decay $K \to \ell\nu$ assuming zero missing mass:

$$m_\ell^2 = (E_K - |\mathbf{p}_K - \mathbf{p}_{\text{d}}|)^2 - \mathbf{p}_{\text{d}}^2. \tag{1.1}$$

The distribution of m_ℓ^2 is shown in Fig. 1 left panel, upper curve, from MC simulation. The muon peak is quite evident, higher masses corresponding to non leptonic and semileptonic decays. No signal of the $K \to e\nu$ (K_{e2}) decay is visible. The very large background around zero mass is the tail of the $K \to \mu\nu$ ($K_{\mu 2}$) peak, due to poor measurements of p_K, $p_{\rm d}$ or the decay angle, $\alpha_{\rm Kd}$. The expected signal from $K_{e2\gamma}$ is also shown in Fig. 1 left, lower curves, separately for $E_\gamma >$10 and $<$10 MeV. The expected number of K_{e2} decays in the sample is $\sim$30,000. A background rejection of at least 1000 is necessary, to obtain a 1% precision measurement of $\Gamma(K_{e2})$, with an efficiency of $\sim$30%.

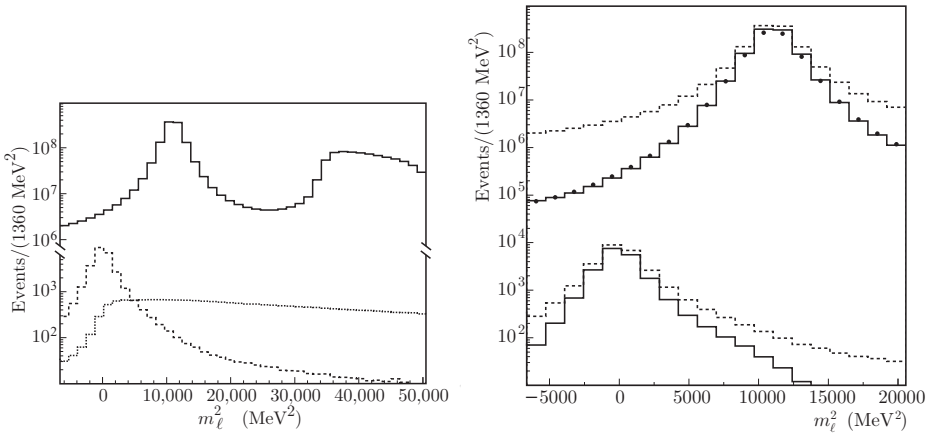

Figure 1: Left: MC distribution of m_ℓ^2, solid line. The contribution of $K_{e2\gamma}$ with $E_\gamma < 10$ MeV (> 10 MeV) is shown by the dashed (dotted) lines. Right: m_ℓ^2 spectrum before (dashed) and after (solid) quality cuts for MC $K_{\mu 2}$ (upper plots)and K_{e2} with $E_\gamma < 10$ MeV (lower plots). Black dots represent data after quality cuts.

The kinematics of the two-body decay $\phi \to K^+K^-$ provides an additional measurement of p_K with ~ 1 MeV resolution, comparable with that from track reconstruction. We require the two p_K determinations to agree within 5 MeV. Further cuts are applied to the daughter track. Resolution of track parameters is improved by rejecting badly reconstructed tracks, i.e., with χ^2(track fit)/ndf$>$ 7.5. Finally, using the expected errors on p_K and $p_{\rm d}$ from tracking, we compute event by event the error on m_ℓ^2, δm_ℓ^2. The distribution of δm_ℓ^2 depends slightly on the opening angle α_{Kd}, which in turn has different distribution for K_{e2} and $K_{\mu 2}$. Events with large value of δm_ℓ^2 are rejected: $\delta m_\ell^2 < \delta_{\rm max}$, with $\delta_{\rm max}$ defined as a function of α_{Kd}, to equalize the losses due to this cut for K_{e2} and $K_{\mu 2}$. The effect of quality cuts on m_ℓ^2 resolution is shown in Fig. 1, right. The background in the K_{e2} signal region is effectively reduced by more than one order of magnitude with an efficiency of $\sim$70% for both K_{e2} and $K_{\mu 2}$.

Information from the EMC is used to improve background rejection. To this purpose, we extrapolate the secondary track to the EMC surface and associate it to a nearby EMC cluster. This requirement produces a signal loss of about 8%. Energy distribution and position along the shower axis of all cells associated to the cluster allow for e/μ particle identification. For electrons, the cluster energy $E_{\rm cl}$ is a measurement of the particle momentum p_d, so that $E_{\rm cl}/p_d$ peaks around 1, while for muons $E_{\rm cl}/p_d$ is on average smaller than 1. Moreover, electron clusters can also be distinguished from μ (or π) clusters by exploiting the granularity of the EMC. All useful information about shower profile and total energy deposition are combined with a 12-25-20-1 structure neural

network trained on $K_L \to \pi\ell\nu$ and $K_{\mu 2}$ data, taking into account variations of the EMC response with momentum and impact angle on the calorimeter. The distribution of the neural network output, *NN*, for a sample of $K_L \to \pi e\nu$ events is shown in Fig. 2 left, for data and MC. Additional separation has been obtained using time of flight information. The data distribution of *NN* as function of

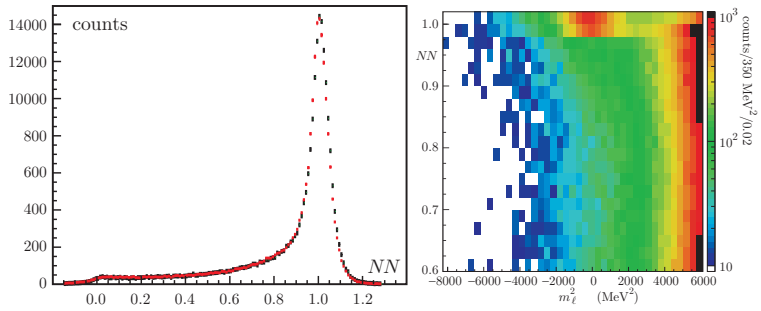

Figure 2: Left: Neural-network output, *NN*, for electrons of a $K_L \to \pi e\nu$ sample from data (black) and MC (red). Right: Data density in the *NN*, m_ℓ^2 plane.

m_ℓ^2 is shown in Fig. 2 right. A clear $K \to e\nu$ signal can be seen at $m_\ell^2 \sim 0$ and $NN \sim 1$.

Some 32% of the events with a K decay in the fiducial volume, have a reconstructed kink matching the required quality criteria *and* an EMC cluster associated to the lepton track; this holds for both K_{e2} and $K_{\mu 2}$. In the selected sample, the contamination from K decays other than $K_{\ell 2}$ is negligible, as evaluated from MC. R_{10}, Eq. 2, is obtained without requiring the presence of the radiated photon. The number of $K \to e\nu(\gamma)$, is determined with a binned likelihood fit to the two-dimensional *NN* vs m_ℓ^2 distribution. Distribution shapes for signal and $K_{\mu 2}$ background are taken from MC; the normalization factors for the two components are the only fit parameters. The fit has been performed in the region $-3700 < m_\ell^2 < 6100$ MeV^2 and $NN > 0.86$. The fit region accepts $\sim 90\%$ of $K \to e\nu(\gamma)$ events with $E_\gamma < 10$ MeV, as evaluated from MC. A small fraction of fitted $K \to e\nu(\gamma)$ events have $E_\gamma > 10$ MeV: the value of this "contamination", $f_{\rm DE}$, is fixed in the fit to the expectation from simulation, $f_{\rm DE} = 10.2\%$. A systematic error related to this assumption is discussed in Sect. 2.

We count 7064 ± 102 $K^+ \to e^+\nu(\gamma)$ events and 6750 ± 101 $K^- \to e^-\bar{\nu}(\gamma)$, 89.8% of which have $E_\gamma < 10$ MeV. The signal-to-background correlation is $\sim 20\%$ and the χ^2/ndf is 113/112 for K^+ and 140/112 for K^-. Fig. 3 shows the sum of fit results for K^+ and K^- projected onto the m_ℓ^2 axis in a signal ($NN > 0.98$) and a background ($NN < 0.98$) region.

The number of $K_{\mu 2}$ events is obtained from a fit to the m_ℓ^2 distribution. The fraction of background events under the muon peak is estimated from MC to be less than one per mil. We count 2.878×10^8 (2.742×10^8) $K^+ \to \mu^+\nu(\gamma)$ ($K^- \to \mu^-\bar{\nu}(\gamma)$) events. The difference between K^+ and K^- counts is due to K^- nuclear interactions in the material traversed.

2. Efficiency and systematic errors evaluation

The ratios of K_{e2} to $K_{\mu 2}$ efficiencies are evaluated with MC and corrected for possible differences between data and MC, using control samples. We evaluate data-MC corrections separately for each of the following analysis steps: decay point reconstruction (kink), quality cuts, cluster-charged particle association. For each step, the correction is defined as the ratio of data and MC

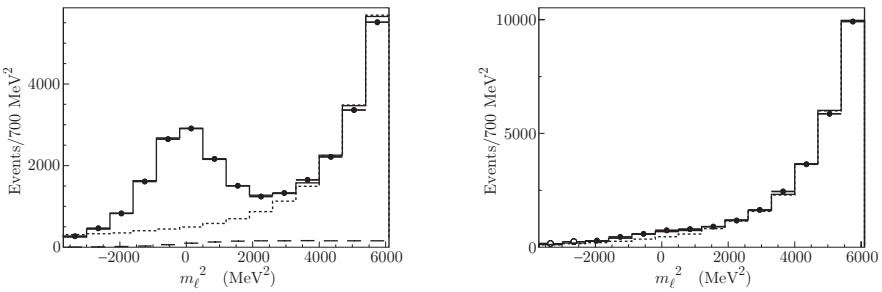

Figure 3: Fit projections onto the m_ℓ^2 axis for $NN > 0.98$ (left) and $NN < 0.98$ (right), for data (black dots), MC fit (solid line), and $K_{\mu 2}$ background (dotted line). The contribution from K_{e2} events with $E_\gamma > 10$ MeV is visible in the left panel (dashed line).

efficiencies measured on the control sample, each folded with the proper kinematic spectrum of K_{e2} (or $K_{\mu 2}$) events.

Decay point reconstruction efficiencies are evaluated using pure samples of $K_{\mu 2}$ and K_{e3}; these are tagged by the identification of the two-body decay, $K_{\mu 2}$ or $K \to \pi\pi^0$ ($K_{\pi 2}$), of the other kaon and selected with tagging and EMC information only, without using tracking. The corrections to MC efficiencies range between 0.90 and 0.99 depending on the decay point position and on the decay angle. The simulation is less accurate in case of overlap between lepton and kaon tracks, and with decays occurring close to the inner border of the fiducial volume.

Samples of $K_L(e3)$, $K_L(\mu 3)$, and $K_{\mu 2}$ decays with a purity of 99.5%, 95.4%, and 100.0% respectively, are used to evaluate lepton cluster efficiencies. These samples are selected using tagging and DC information only, without using calorimeter, see Refs. [9]. The efficiency has been evaluated as a function of the particle momentum separately for barrel and endcap. The correction to MC efficiencies ranges between 0.98 and 1.01 depending on the momentum and on the point of impact on the calorimeter. The trigger efficiency has been evaluated solely from data.

The absolute values of all of the systematic uncertainties on R_{10} are listed in Table 1. All of the sources of systematic error are discussed below.

		$\delta(R_{10})\times 10^5$
Statistical error		0.024
Systematic error		
Counting:	fit	0.007
	DE	0.005
Efficiency:	kink	0.014
	trigger	0.009
	e,μ cluster	0.005
Total systematic error		0.019

Table 1: Summary of statistical and systematic uncertainties on the measurements of R_{10}.

To minimize possible biases on K_{e2} event counting due to the limited knowledge of the momentum resolution, we used $K_{\mu 2}$ data to carefully tune the MC response on the tails of the m_ℓ^2 distribution. This has been performed in sidebands of the *NN* variable, to avoid bias due to the

presence of K_{e2} signal. Similarly, for the *NN* distribution the EMC response in the MC has been tuned at the level of single cell, using $K_{\ell 3}$ data control samples. Residual differences between data and MC K_{e2} and $K_{\mu 2}$ *NN* shapes have been corrected by using the same control samples. Finally, to evaluate the systematic error associated with these procedures, we studied the variation of the results with different choices of fit range, corresponding to a change of overall purity from $\sim 75\%$ to $\sim 10\%$, for $K \to e\nu(\gamma)$ with $E_\gamma < 10$ MeV. A systematic uncertainty of $\sim 0.3\%$ is derived by scaling the uncorrelated errors so that the reduced χ^2 value equals unity (see also Table 1).

K_{e2} event counting is also affected by the uncertainty on $f_{\rm DE}$, the fraction of K_{e2} events in the fit region which are due to DE process. This error has been evaluated by repeating the measurement of R_{10} with values of $f_{\rm DE}$ varied within its uncertainty, which is $\sim 4\%$ according to our measurement of the $K_{e2\gamma}$ differential spectrum [7]. Since the m_ℓ^2 distributions for $K_{e2\gamma}$ with $E_\gamma < 10$ MeV and with $E_\gamma > 10$ MeV overlap only partially, the associated fractional variation on R_{10} is reduced: the final error due to DE uncertainty is 0.2% (Table 1).

Different contributions to the systematic uncertainty on $\varepsilon_{e2}/\varepsilon_{\mu 2}$ are listed in Table 1. These errors are dominated by the statistics of the control samples used to correct the MC evaluations. In addition, we studied the variation of each correction with modified control-sample selection criteria. We found neglible contributions in all cases but for the kink and quality cuts corrections, for which the bias due to the control-sample selection and the statistics contribute at the same level.

The total systematic error is $\sim 0.8\%$, to be compared with statistical accuracy at the level of $\sim 1\%$.

3. R_K and lepton-flavor violation

The number of $K \to e\nu(\gamma)$ events with $E_\gamma < 10$ MeV, the number of $K \to \mu\nu(\gamma)$ events, the ratio of K_{e2} to $K_{\mu 2}$ efficiencies and the measurement of R_{10} are given in Table 2 for K^+, K^- and both charges combined. K^+ and K^- results are consistent within the statistical error. The systematic uncertainty is common to both charges.

	N(K_{e2})	N($K_{\mu 2}$)	$\varepsilon_{e2}/\varepsilon_{\mu 2}$	$R_{10} \times 10^5$
K^+	$6348 \pm 92 \pm 23$	2.878×10^8	$0.944 \pm 0.003 \pm 0.007$	$(2.336 \pm 0.033 \pm 0.019)$
K^-	$6064 \pm 91 \pm 22$	2.742×10^8	$0.949 \pm 0.002 \pm 0.007$	$(2.330 \pm 0.035 \pm 0.019)$
$K^\pm$	$12412 \pm 129 \pm 45$	5.620×10^8	$0.947 \pm 0.002 \pm 0.007$	$(2.333 \pm 0.024 \pm 0.019)$

Table 2: Number of K_{e2} and $K_{\mu 2}$ events, efficiency ratios and results for R_{10} for K^+, K^-, and both charges combined; first error is statistical, second one is systematic.

To compare the R_{10} measurement with the inclusive R_K prediction from SM, we take into account the acceptance of the 10 MeV cut for IB, Eq. 3. We obtain: $R_K = (2.493 \pm 0.025_{\rm stat} \pm 0.019_{\rm syst}) \times 10^{-5}$, in agreement with SM prediction of Eq. 1. In the framework of MSSM with lepton-flavor violating (LFV) couplings, R_K can be used to set constraints in the space of relevant parameters, using the following expression [3]:

$$R_K = R_K^{\rm SM} \times \left[1 + \left(\frac{m_K^4}{m_H^4}\right)\left(\frac{m_\tau^2}{m_e^2}\right)\left|\Delta_R^{31}\right|^2 \tan^6\beta\right], \qquad (3.1)$$

where M_H is the charged-Higgs mass, Δ_R^{31} is the effective e-τ coupling constant depending on MSSM parameters, and $\tan\beta$ is the ratio of the two Higgs superfields vacuum expectation values. The regions excluded at 95% C.L. in the plane M_H–$\tan\beta$ are shown in Fig. 4 for different values of the effective LFV coupling Δ_R^{31}.

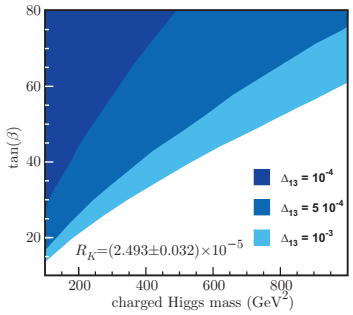

Figure 4: Excluded regions at 95% C.L. in the plane M_H–$\tan\beta$ for $\Delta_R^{31} = 10^{-4}, 5\times10^{-3}, 10^{-3}$.

4. Conclusions

We have performed a comprehensive study of the process $K_{e2\gamma}$. We have measured the ratio of $K_{e2\gamma}$ and $K_{\mu2}$ widths for photon energies smaller than 10 MeV, without photon detection requirement. We find: $R_{10} = (2.333 \pm 0.024_{\text{stat}} \pm 0.019_{\text{stat}}) \times 10^{-5}$. From this result we derive the inclusive ratio R_K to be compared with the SM prediction: $R_K = (2.493 \pm 0.025_{\text{stat}} \pm 0.019_{\text{syst}}) \times 10^{-5}$, in excellent agreement with the SM prediction $R_K = (2.477 \pm 0.001) \times 10^{-5}$. Our result improves the accuracy with which R_K is known by a factor of 5 with respect to the present world average and allows severe constraints to be set on new physics contributions in the MSSM with lepton flavor violating couplings.

References

[1] W.J. Marciano and A. Sirlin, *Phys. Rev. Lett.* **71** (1993) 3629; M. Finkemeier, *Phys. Lett. B* **387** (1996) 391.

[2] V. Cirigliano and I. Rosell, *Phys. Rev. Lett.* **99** (2007) 231801.

[3] A. Masiero, P. Paradisi and R. Petronzio, *JHEP* **0811** (2008) 042

[4] J. Bijnens, G. Colangelo, G. Ecker and J. Gasser, [hep-ph/9411311].

[5] J. Heintze *et al.*, *Nucl. Phys. B* **149** (1979) 365.

[6] N. Cabibbo, *Phys. Rev. Lett.* **10** (1963) 531.

[7] See M. Moulson contribution in these proceedings.

[8] C. Gatti, *Eur. Phys. J. C* **45**, 417 (2006).

[9] F. Ambrosino *et al.*, KLOE Coll., *Phys. Lett., B* **632** (2006) 43-50; F. Ambrosino *et al.*, KLOE Coll., *Phys. Lett. B* **636**, 166 (2006); F. Ambrosino *et al.*, KLOE Coll., *JHEP* **12** (2007) 105

[10] M. Antonelli *et al.* arXiv:0801.1817 [hep-ph].